JAAS
Journal of Analytical Atomic Spectrometry

Accepted Manuscript

This article can be cited before page numbers have been issued, to do this please use: D. Friebel, T. Vogt and C. Vogt, *J. Anal. At. Spectrom.*, 2026, DOI: 10.1039/D6JA00173D.

View Article Online
DOI: 10.1039/D6JA00173D

Process-accompanying analysis of solid intermediate and end products in the manufacturing process of high-purity tungsten by ETV-ICP-OES

Dina Friebel[a], Thomas Vogt*[a], Carla Vogt[a]

[a] Institute of Analytical Chemistry, TU Bergakademie Freiberg, Leipziger Str. 29, 09599 Freiberg, Germany

E-Mail addresses:
M.Sc. Dina Friebel: Dina.Friebel@extern.tu-freiberg.de

Dr. rer. nat. Thomas Vogt: Thomas.Vogt@chemie.tu-freiberg.de

Prof. Dr. rer. nat. habil. Carla Vogt: Carla.Vogt@chemie.tu-freiberg.de

Author note:

* Correspondence concerning this research paper should be addressed to Dr. rer. nat. Thomas Vogt, Institute of Analytical Chemistry, TU Bergakademie Freiberg, Leipziger Str. 29, 09599 Freiberg, Germany, Tel.: +49 3731 392335, E-Mail address: Thomas.Vogt@chemie.tu-freiberg.de

Dina Friebel https://orcid.org/0000-0001-8256-2741

Thomas Vogt https://orcid.org/0000-0002-1115-3286

Carla Vogt https://orcid.org/0000-0002-6711-0103

Keywords:

multi element analysis

tungsten and tungsten compounds

ETV-ICP-OES

solid sampling

matrix-independent calibration

trace analysis in solid materials

Analysis of high-purity tungsten

View Article Online
DOI: 10.1039/D6JA00173D

Abstract

Many solids from the production of high-purity tungsten are challenging to analyze due to their insolubility and tungsten's high spectral line density, which causes interferences in many spectroscopic methods. To address this, electrothermal vaporization (ETV) coupled with inductively coupled plasma optical emission spectrometry (ICP-OES) was optimized for the direct multi-element analysis of various tungsten-based materials, including ammonium paratungstate ($(NH_4)_{10}(H_2W_{12}O_{42}) \cdot 4\ H_2O$), yellow tungsten oxide (WO_3), blue tungsten oxide (WO_{2+x}), tungsten metal powder (W) and tungsten carbide (WC). The method focused on detecting critical contaminants like Al, B, P, S and Si as well as O in W and WC, which affect the characteristics of final products. The optimization includes the selection of suitable plasma parameters and emission lines. Since, for example, almost all emission lines of the important element sulfur are interfered by tungsten, a way had to be found to separate the analytes from its matrix. With the assistance of hydrogen as a reaction gas and temperatures up to 2400 °C, the analytes can be vaporized while the tungsten matrix remains in the graphite boats of the ETV unit. Since no suitable certified reference materials were available, a calibration using dried liquid ICP standard solutions was tested successfully.

View Article Online
DOI: 10.1039/D6JA00173D

Introduction

Analyzing impurities in chemically stable solid samples at low concentrations (mg/kg to µg/kg) is challenging for most analytical methods. While optical emission spectrometry or mass spectrometry are often used, their typical sample introduction systems are limited to liquids.[1] Solid samples like plastics, metals, rocks, ceramics, or graphite require time-consuming and often hazardous dissolution procedures, frequently involving highly toxic chemicals like hydrofluoric acid.[2,3] This process can introduce contamination and necessitate dilutions that push element concentrations below detection limits.

Direct analysis of solid samples is preferred for ecological, economic, and technical reasons. An ideal method would require no sample preparation, offer short measurement times, and have a high dynamic range to minimize contamination risks and the need for toxic chemicals, making it suitable for routine process analysis.

Production Process of tungsten and tungsten compounds

For various manufacturing processes, such as cutting, engraving or grinding, materials are required that are harder than the material of the workpiece. Diamonds, which are frequently used for cutting tools, wire drawing stones and rock drills, have the highest degree on the Mohs scale of mineral hardness. However, since diamonds have a comparatively low fracture strength, alternative hard materials are needed. Desired properties of a suitable material include the highest possible hardness, wear and fracture resistance, thermal stability, thermal shock resistance, thermal conductivity and chemical stability.[1,4,5]

A hardness similar to diamond is obtained with metal-rich, electrically conductive nitrides and carbides. These are already being produced for cutting tools, refractory coatings, thermocouples, and other applications. One of the most prominent representatives of this class of materials is a sintered hard metal made of tungsten carbide and 10 % cobalt. It is used, for example, for processing cast iron, non-ferrous metals, plastics, wood or rocks.[4,6,7]

In order to obtain the required hardness, a high purity of the tungsten carbide is required. Elements such as aluminium, oxygen, phosphorus, sulfur or silicon or can influence the metal in terms of its ductility to such an extent that it becomes brittle and can no longer be used as a tool for machining.[8-10] For instance, doping blue tungsten oxide as a raw material for a sintered heavy alloy (90% W, 7 % Ni and 3 % Fe) with 100 $mg \cdot kg^{-1}$ Al (40 $mg \cdot kg^{-1}$ in the resulting tungsten powder) reduces the tensile strength from 923 to 769 MPa and the elongation from 24 to 4 %.[5] Similar trends were reported for phosphorous and sulfur. The addition of 50 $mg \cdot kg^{-1}$ of boron to the oxide, on the other hand, increases the tensile strength from 994 to 1009 MPa and the elongation from 22 to 28 %.[5]

Metallic tungsten is extracted from the ores wolframite ($(Mn,Fe)WO_4$) and scheelite ($CaWO_4$), whereby wolframite does not exist as an independent mineral, but describes a mineral mixture of hübnerite ($MnWO_4$) and ferberite ($FeWO_4$). The raw materials are ground, concentrated by flotation, and refined by reaction with sodium carbonate or by pressure leaching with sodium hydroxide. The sodium tungstate (Na_2WO_4) formed is

View Article Online
DOI: 10.1039/D6JA00173D

purified by various steps including extractions and ion exchange and converted to trioxide monohydrate ($WO_3 \cdot H_2O$) by acidification. For further purification, the oxide is leached with ammonia solution and precipitated as ammonium paratungstate ($(NH_4)_{10}(H_2W_{12}O_{42}) \cdot 4\ H_2O$, abbreviated as APT).[4,11,12]

Along the production process, the analysis starts at the intermediate APT since the preliminary products go through several purifying steps. In case of containing a too high amount of contamination, APT can be added to sodium tungstate to go through the purification process again before the energy-consuming steps of the reduction to tungsten oxide and tungsten will be performed. The tungsten oxides WO_3 (yellow tungsten oxide) and WO_{2+x} (blue tungsten oxide) can be obtained by thermal decomposition at 600 °C. The oxides are finally reduced to the metal at 800 °C in a hydrogen atmosphere yielding a tungsten powder with a purity greater than 99.9 %. High purity tungsten carbide can be produced by reacting high purity tungsten with high purity graphite. The reaction is carried out at 1500 °C either under hydrogen atmosphere in an electric resistance furnace or under vacuum in an induction furnace. [4,11,12]

State of the art for the analysis of tungsten-based materials

Many industrial intermediate and end products occur as solids in the form of powder or granules, for which direct analyzation techniques are limited.[1] The analysis of the elemental composition of solids is still a major challenge, especially when contaminants in the trace element range are to be analyzed. Methods like ICP-OES or ICP-MS need a time-consuming sample preparation, such as digestion processes.[2,3]

In order to circumvent the highly corrosive and caustic hydrofluoric acid, different solvent combinations have been explored. Hydrogen peroxide, as well as a mixture of H_3PO_4 and HNO_3 (1:5) are also capable of dissolving metallic tungsten, tungsten carbide or a WC-Co based cemented carbide.[6,13-15] Moreover, mixtures of ammonia and ammonium citrate and of ammonia and tartaric acid are capable of dissolving tungsten-containing compounds. Ammonia as well as sodium hydroxide dissolve tungsten trioxide to form tungstates. The addition of tartaric acid or even oxalic acid serves to complex the metal to keep it in solution.[6,11] Typical analytical methods for tungsten-based materials include ICP-OES, ICP-MS and AAS.[13,16,17] Cheng *et al.*[13] obtained detection limits between 4 $\mu g \cdot L^{-1}$ for Nb to 13 $\mu g \cdot L^{-1}$ for Fe in dissolved tungsten compounds, with relative standard deviations (RSD) lower than 3 % and recovery rates from 97.0 % to 103.5 %. However, it should be noted that the use of organic solvent or complexing agents might result in complex matrix effects and interferences within a plasma and are therefore problematic for analyses using ICP-OES or ICP-MS.[18,19]

Comparatively little is published about the solubility of ammonium paratungstate. It is known that it dissolves like WO_3 in sodium hydroxide solution.[20] Dissolution experiments in acid, as typically used in microwave-assisted digestion processes, have not been reported so far.

The high density of emission lines of tungsten is still a problem, when the samples are brought into solution, because this frequently causes interferences with the emission lines of the analytes. Since the digestion procedures are time-consuming, the results are time-delayed and the method cannot be used to accompany the process.

View Article Online
DOI: 10.1039/D6JA00173D

To minimize the risk of contamination and to avoid toxic high purity chemicals, direct solid-sampling methods are preferred. In case of optical spectroscopy, the complex emission spectrum of the matrix remains problematic. Furthermore, the numerous gamma ray emitting isotopes of tungsten limit the use of methods like neutron activation analysis (NAA), which is also not suitable for process-accompanying analyses.[21] Nevertheless, Cosgrove *et al.* applied gamma scintillation spectroscopy to tungsten and tungsten oxides reaching detection limits in the range of 0.1 mg·kg^{-1}, recovery rates from 70 to 100 % for most elements and accuracy and precision within about 1 %.[21]

As methods to analyse solid samples directly, X-ray fluorescence spectroscopy (XRF) or glow discharge mass spectrometry (GD-MS) can be applied, respectively.[13,16,20] X-ray fluorescence analysis (XRF) is widely used in industry, but it quickly reaches its limits when analysing light elements or concentrations below mg·kg^{-1}.[1] Therefore, the method is only suitable for the determination of major and minor elements down to the ppm range, but not for ultratrace analysis and not for lighter elements.[1,17,22,23]

Methods with low limits of detection such as secondary ion mass spectrometry (SIMS), glow discharge mass spectrometry (GD-MS) or laser ablation as a sample introduction system for a mass analyser or an optical emission spectrometer (LA-ICP-MS or -OES) are only suitable for samples with a firm and smooth surface.[24- 27] The analysis of powder samples or granules is only possible if a sample preparation like pressing a pellet is carried out. For GD-MS, most pressed powder samples cannot withstand the necessary high vacuum, and are poorly electrically conductive. Therefore, the method cannot be applied to process products like ammonium paratungstate and tungsten oxide. Otherwise, GD-MS is characterized by detection limits down to 0.1 µg·kg^{-1}, a large linear range, and high reproducibility.[27] In addition, a major advantage is that a calibration with non-matrix standard reference materials is usually unproblematic. However, because a high-resolution mass spectrometer is required, the method is very expensive. Since GD-MS cannot be automated with a sample changer, it is rather unsuitable for routine in-process analyses. Nevertheless, GD-MS is widely used in industry for the analysis of tungsten metal. [24-27]

Another possibility for analysing solids with detection limits in the ppb range (0.001 - 0.1 mg·kg^{-1})[27] is secondary ion mass spectrometry (SIMS). The method is well suited for the analysis of metals containing tungsten. However, powder samples can only be analyzed by complex sample preparation, with the risk of sample contamination. Again, the possibility of in-process use as a routine method is not given.[1,8,22]

In addition to the surface properties of the material, the matrix itself presents as a problem for many analytical methods. Especially in samples with a high organic content, in salts, rocks or ceramics, various elements are already contained in the matrix, whose emission or fluorescence lines lead to spectral interferences and increased backgrounds in the recorded spectra.[16,17] Some metals, primarily tungsten and molybdenum, already contribute to significant interference effects through their own enormous spectral line density in emission spectrometry. In these cases, an analysis of trace or ultratrace elements is only possible if the analytes can be separated from the matrix with the exclusion of contamination and dilution effects.

View Article Online
DOI: 10.1039/D6JA00173D

Electrothermal vaporization as a sample introduction system for ICP-OES

A highly efficient analytical method for direct qualitative and quantitative multi-element analysis of solids is the electrothermal vaporization (ETV) as a sample introduction system for atomic emission spectrometry (ICP-OES). The method has already been used to analyse poorly soluble matrices and was now applied to tungsten-based materials.

The samples are introduced to the longitudinally heated graphite furnace of the ETV unit within a graphite boat (see fig. 1). With the help of a modifier gas, the sample is evaporated with temperatures up to 2500 °C. By using a modifier gas, even non-volatile samples can be vaporized. Common modifiers usually contain halogens to secure complete evaporation, i.e. Dichlorodifluoromethane (CCl_2F_2), Fluoroform/Trifluoromethane (CHF_3), Tetraflouromethane (CF_4), Sulfur hexafluoride (SF_6) or Nitrogen trifluoride (NF_3).[23,28,29] Non-volatile components or elements, that tend to form carbides, can still be completely evaporated with the help of such reactive gases due to the forming of halogenites. Therefore, it is possible to analyze substances such as glass[30], ceramics[31-35], boron nitride[36,37] or silicon carbide[38-40] with ETV-ICP-OES. With the help of a carrier gas, which usually consists of argon, the sample can be carried to any kind of optical emission spectrometer with a high efficiency. This is achieved by a cool bypass gas (argon), which laminar flows around the hot gas of sample and argon from the furnace, immediately after passing the nozzle. As a result, condensation on cold surfaces can be avoided and a dry aerosol is generated, which can be almost completely transferred into the plasma. Depending on the element, a transport efficiency of over 90 % can be achieved.[23] The ETV allows the temperature profile to be freely programmed so that optimum evaporation can be achieved for different matrices. Usually, even the matrix will be evaporated using halogen containing modifiers which causes disadvantages in case of tungsten samples.

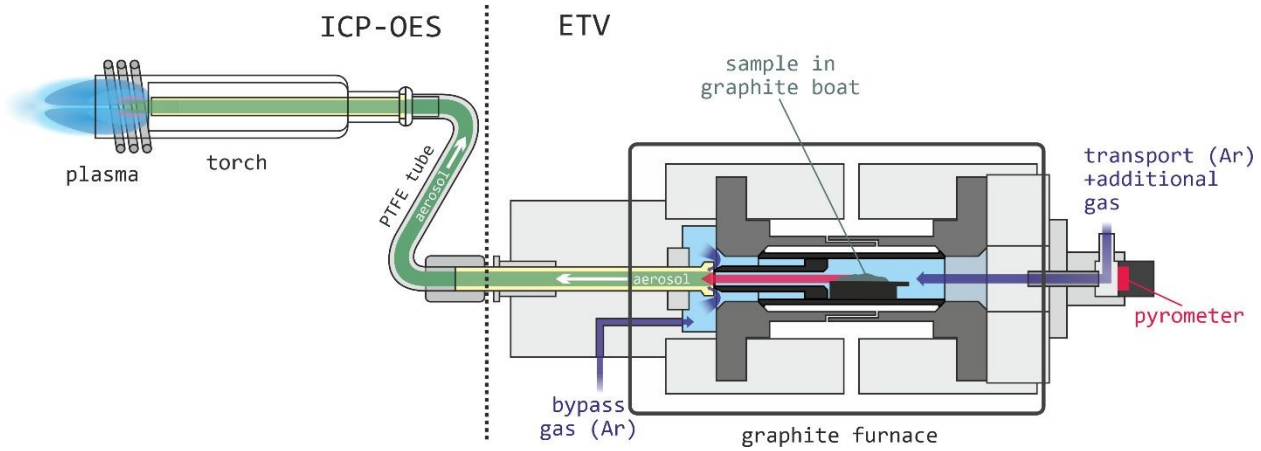

Figure 1: Schematic construction of the graphite furnace of the ETV unit

The coupling with an ICP spectrometer is realized via a PTFE or PFA tube. The dry aerosol containing the sample and argon is carried to the plasma torch of the spectrometer, where dissociation, excitation and emission of element-specific radiation takes place. To detect the emission, either a spectrometer with Echelle or Rowland circle optic can be used, although less interference is observed with the Rowland circle since the interferences caused by blooming, which describes the overlapping of diffraction orders by very intense signals, are eliminated. Within the Rowland circle, a holographic grid serves as the dispersing element, which

View Article Online
DOI: 10.1039/D6JA00173D

divides the radiation into its individual wavelengths and focuses them at the same time. The radiation is detected by CCD line detectors arranged on a circle.

Basic considerations of the ETV-ICP-OES method for tungsten-based materials

The enormous spectral line density of tungsten causes strong interferences in optical emission spectroscopy when samples containing tungsten are analyzed. For instance, the most intense emission lines of sulfur at 182.034 and 180.731 nm are completely overlapped by emission lines of tungsten. To perform analysis of products along the production of high-purity tungsten, a method needs to be developed to separate the analytes from the matrix. When halogenated modifier gases such as CCl_2F_2 or CHF_3 are used, volatile tungsten halides are formed that cause interferences. Therefore, an evaluation is needed to see if the analytes can be separated from the matrix with low heating rates. The idea was to evaporate highly volatile analytes such as sulfur and phosphorus at lower temperatures than the evaporation temperatures of the halogenated tungsten compounds. If separation at low heating rates does not show the desired results, the samples can also be heated entirely without modifier gas, with the expectation that tungsten, which only evaporates at very high temperatures, will remain in the graphite boat of the ETV and only the analytes will be vaporized. The problem with this method might be that the analytes remain in the matrix, or that the vaporization causes a carryover of the matrix into the plasma.

An alternative might be the use of hydrogen as a modifier gas.[28,41] Comparable to the production process of tungsten, the tungsten compounds APT and WO_3 are reduced to tungsten. During the conversion to the metal, the analytes are expected to be thermally released from the matrix and transported into the plasma of the ICP-OES spectrometer. The tungsten matrix should remain in the graphite boat of the ETV, which should eliminate most of the optical interferences causes by tungsten. A careful selection of emission lines used for evaluation will also help to minimize the interferences between the analytes. Whether the method works also in case of already reduced metallic tungsten and tungsten carbide, needs to be evaluated.

When the matrix is not introduced into the plasma, the calibration method is not required to be matrix-analogous. Calibration is also possible with other solid reference materials or ICP liquid standards that are pipetted into the graphite boat and dried.[42] This is an advantage in this and many other cases, as matrix-matched standards are not available for many matrices.

Experimental section

Instrumentation

The investigations were performed using the ICP-OES spectrometer ARCOS EOP from SPECTRO Analytical Instruments GmbH (Kleve, Germany). For sample introduction, the system was interfaced via a PTFE-transport tubing to the solid sampling electrothermal vaporization unit ETV 4000c from Spectral Systems (Fürstenfeldbruck, Germany).

Analysis of high-purity tungsten

Initially, the halogenated gases CCl_2F_2, CHF_3 and NF_3 were tested as modification gases with and without plasma humidification, and low heating rates were applied to separate the analytes from the tungsten matrix. Additionally, tests without the use of a modifier gas were carried out. Furthermore, the use of hydrogen as a modifier, as Hassler *et al.*[28,29] described for the analysis of high-purity copper, was tested. The method was adapted to the analysis of tungsten-based materials. The hydrogen flow rate was increased to 80 mL·min^{-1} in comparison to the flowrate of halogenated modifiers which is usually set around 2.2 mL·min^{-1}. The sum of modifier gas flow rate and inner gas flowrate is usually set at about 140 to 150 mL·min^{-1} to ensure laminar flow of the bypass gas. Therefore, the inner gas flow rate was reduced to 60 mL·min^{-1}. Due to the usage of hydrogen, the plasma temperature increases. Therefore, the ICP plasma RF power has to be decreased or the coolant gas flow rate has to be increased. The RF power was varied between the technical possible 1200 to 1650 W and combined with an increasing coolant gas flow from 14 to 18 L·min^{-1}. It was observed, that the plasma gets instable if the power was lower than 1400 W and the intensity of the considered emission lines increase with increasing RF power. In order not to lose the signal intensity through to a lower plasma power, the coolant gas flow was increased from typically 16.5 L·min^{-1} to 18 L·min^{-1}. The optimized technical parameters for the analysis with H_2 as a modifier are presented in table 1 while the wavelengths selected for the analyzed elements can be found in table 2.

Table 1: Optimized working parameters of the instruments

Instrument	Parameter	Value
ETV	Modifier gas (H_2) flow rate	80 mL·min^{-1}
	Bypass-gas (Ar) flow rate	400 mL·min^{-1}
	Inner gas (Ar) flow rate	60 mL·min^{-1}
	Temperature program	20-100 °C (5 s)
		100 °C (25 s)
		100 – 2350 °C (50 s)
		2350 – 2400 °C (20 s)
		2400 – 20 °C (20 s)
ICP	ICP plasma RF-power	1650 W
	Coolant gas flow rate	18.0 L·min^{-1}
	Plasma gas flow rate	1.60 L·min^{-1}
OES	Mounting	Paschen Runge
	Detector	CCD array
	Wavelength range	130-770 nm
	Plasma observation	axial

View Article Online
DOI: 10.1039/D6JA00173D

Table 2: Selected wavelengths and integration intervals of the investigated elements

Element	Wavelength [nm]	Alternative wavelength [nm]	Integration interval [s]	Total integration time [s]
Al	396.152	167.078	55-100	45
As	189.042	228.812	30-85	55
B	249.773	249.677	30-100	70
Mn	259.373	260.569	50-105	55
O	130.603	130.485	30-65	35
P	177.495	213.618	35-90	55
S	182.034	180.731	35-85	50
Si	288.158	251.612	30-105	75

Samples and preparation

To create a calibration curve, the graphite boats of the ETV were cleaned in the graphite oven with temperatures up to 2450 °C. The cleaning step was performed just prior to the analysis in order to keep the contaminating effect from the laboratory atmosphere low. The samples were then weighted in the graphite boats of the ETV using a precision balance by Mettler Toledo (XPR105 DR, Gießen, Germany) with an accuracy of 0.01 mg. To minimize contaminations, the samples were transferred by disposable antistatic spatulas (VWR, 14 mm length, 3 mm tip). The samples were analyzed in triplicate.

For calibration, the applicability of graphite reference materials and dried aqueous standard solutions were tested. As graphites, BAM S009 and an inhouse graphite standard material were tested with sample masses between 0.5 and 5 mg. For liquid calibration, 1000 mg·L^{-1} single element ICP standard solutions were mixed and diluted to solutions of 10 mg·L^{-1} and 1 mg·L^{-1}. The standard solutions for Al and As were purchased from Alfa Aeser in 5 % HNO_3. For B and Mn Merck Certipur standard solutions were applied. P and S were used as ammonium compounds from the sample line Roth RotiStar. Si was bought as a solution in 1 M HNO_3 and 2 % HF from Fluka. The diluted solutions (5 and 10 µL of the 1 mg·L^{-1} solution and 2-40 µL of the 10 mg·L^{-1} solution) were pipetted into cleaned graphite boats and dried at 70 °C on a ceramic heating plate.

To calibrate the oxygen mass fractions, six graphite boats were loaded with 0.1 to 1 mg calcium oxalate monohydrate ($CaC_2O_4 \cdot H_2O$; Carl Roth, > 98 %, mass: 146.12 g·mol^{-1}). Since the CaO is evaporated at higher temperatures (> 1800 °C) as the release of oxygen in the samples (150 – 1500 °C) there are only four oxygen ions left to be evaporated during the integration interval (see tab. 2). Therefore, for calculation, the compound contains 43.8 % of oxygen.

As samples, several compounds along the production process of tungsten were chosen. The analysis was started with ammonium paratungstates ($(NH_4)_{10}(H_2W_{12}O_{42}) \cdot 4\ H_2O$), was continued with blue tungsten oxides (WO_{3-x}) and yellow tungsten oxides (WO_3) and ended with the final products metallic tungsten (W) and tungsten carbides (WC). The manufacturers of the provided samples asked to remain anonymous.

View Article Online
DOI: 10.1039/D6JA00173D

Since the method development was not based on certified reference materials, due to a lack thereof, about 10 mg of one sample of each APT, WO_3 as well as W was spiked with the considered elements in form of a standard addition procedure (2, 5 and 10 µL of the 1 mg·L^{-1} solution; 2, 5, 10, 15 and 20 µL of the 10 mg·L^{-1} solution). Liquid ICP standard solutions were added to the samples in the graphite boats and dried at 70 °C on a ceramic heating plate. Doping higher samples masses with the elements of interest and milling them to receive homogenous samples was avoided to prevent contamination.

Results and discussion

Modifier gas

Due to the spectral diversity of tungsten, numerous emission lines of analytes of interest are interfered with, such as almost all emission lines of sulfur. Therefore, a way had to be found to separate the analytes from the matrix. Halogenated modifier gases are commonly used to evaporate non-volatile compounds or elements that tend to form carbides. For tungsten analysis, the difference in the boiling points of tungsten and tungsten carbide (> 5500 °C) and tungsten chlorides and fluorides (< 500°C) could be exploited.[4] Several modifiers and temperature programs with different heating rates were applied in order to evaporate the analytes of interest sequentially. As modifier gases, at first the usual halogenated gases CCl_2F_2 and CHF_3 were tested and low heating rates (< 40 K·s^{-1}) were applied to separate the analytes from the tungsten matrix. The time resolved spectra did not show the expected results and tungsten was evaporated before the analytes, as demonstrated in figure 2 for two sulfur emission lines when CCl_2F_2 was used as a modifier. The reaction gases SF_6 and NF_3 were considered as modifiers to generate a different release behavior from the matrix, but a separation of analytes and matrix was still not possible. The low boiling points of halogenated tungsten compounds made the separation impossible while the emission lines that are not interfered with by tungsten are not intense enough to be used for trace or ultratrace analysis.

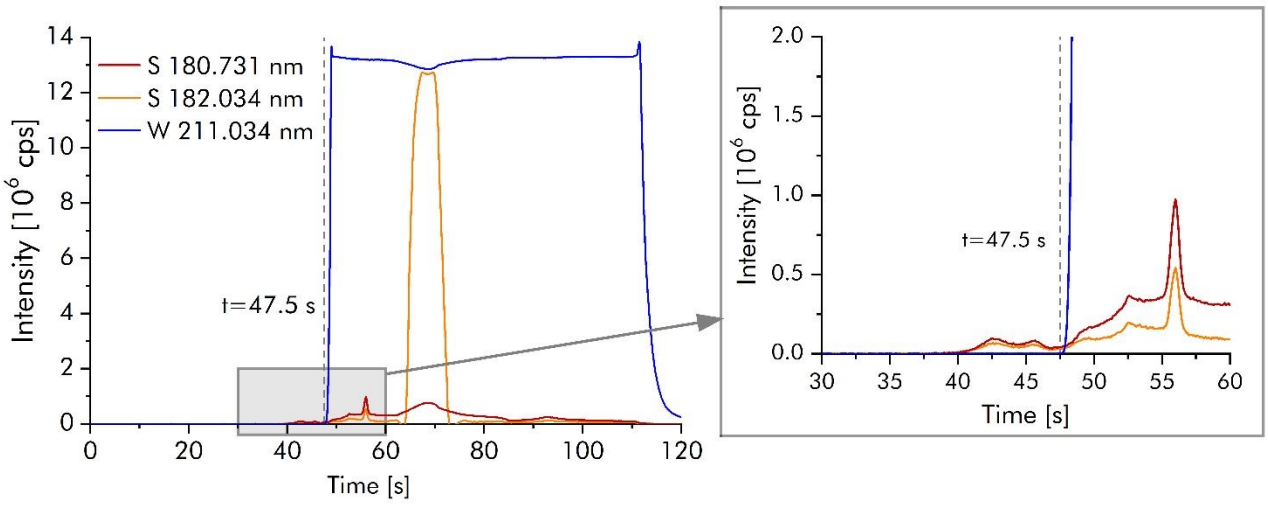

Figure 2: Selected emission lines of sulfur and tungsten using CCl_2F_2 as a modifier gas (2 mg WO_3, 7 ppm S, heating rate of 38.3 K · s^{-1} in the magnified area)

Therefore, a method was developed that does not evaporate tungsten at all. First, no modifier gas was used, but there was still a certain amount of tungsten matrix introduced to the plasma. Since Hassler *et al.*[28,29]

View Article Online
DOI: 10.1039/D6JA00173D

described the use of hydrogen as a modifier gas for the analysis of high-purity copper, the method was adapted to tungsten-based materials. With the help of hydrogen, the analytes can be completely removed while the matrix remains in the graphite boats of the ETV. Therefore, tungsten emission lines will not interfere with the lines of the analytes (figure 3, blue/purple), while a noticeable interference (orange) can be observed using halogenated modifiers. The full spectra of all selected elements are presented for the different sample types in figure S.1 in the electronic supplementary information.

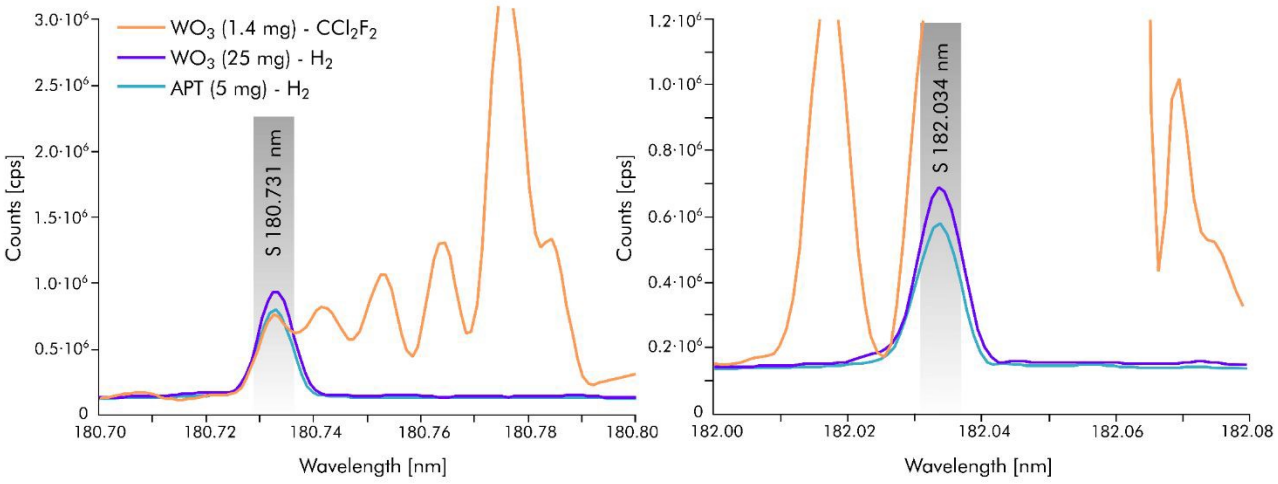

Figure 3: Comparison of interferences on two sulfur emission lines in presence of different tungsten containing matrices using CCl_2F_2 and H_2 as modifier gases at 2400 °C

When ammonium paratungstate and tungsten oxides are used as samples, it has been demonstrated that all analytes can be completely removed from the matrix with a constant heating rate up to 2000 °C. In case of tungsten or tungsten carbide, as shown in figure 4 for the example of phosphorous, the release is found to be incomplete when the temperature program up to 2000 °C (see fig. 4, program **A**) is applied. Consequently, elevated temperatures of up to 2400 °C (see fig. 4, program **B**) are required to ensure the complete removal of the analyte. The transient signals of a representative of all sample types are given for the selected elements in figure S.2 in the electronic supplementary information.

View Article Online
DOI: 10.1039/D6JA00173D

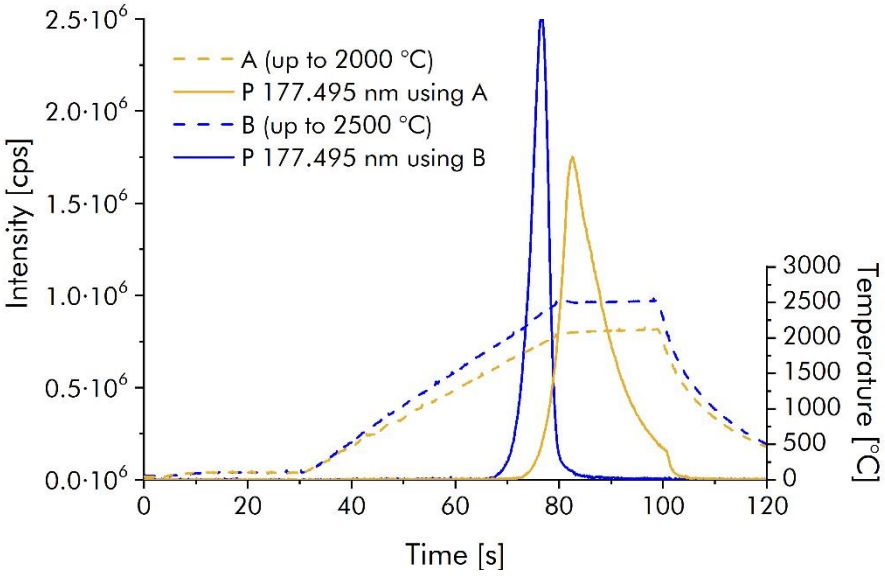

Figure 4: Transient signals of the emission line of phosphorous at 177.495 nm in WC with different maximum temperatures (**A**- orange curve, temperature up to 2000 °C, incomplete removal; **B**- blue curve, temperature up to 2400 °C, complete removal)

Since only the evaporated analytes reach the ICP, higher sample weights can be used without overloading the plasma. To compensate homogeneity issues and generate low limits of detection, sample weights of about 25 mg are recommended for the analysis of the tungsten materials without causing a detector overflow. This is about 5 to 100 times more than the sample mass that can be used for ETV-ICP-OES in case of glass, coal or biomass.[23,30,42-46] In case of samples with extremely low amounts of certain elements of interest, the sample weight can also be increased up to 40 mg if needed. To analyse samples containing comparatively high amounts of contaminating elements, the sample weight can be reduced to 5 mg. In this case, it might also be beneficial to switch to emission lines with lower intensities, for instance using the emission line of phosphorous at 138.147 nm instead of the lines at 177.495 and 213.618 nm or the emission line of sulfur at 142.503 nm instead of the lines at 182.034 and 180.731 nm. As a general recommendation, these emission lines with lower intensities should be included in the measurement program.

The tungsten matrix that remains in the graphite boats even keeps most of the original structure while the analytes are evaporated, resulting in a sponge-like constitution of the residues as shown in the SEM images in figure 5. Additional images are presented in figures S.3.1 – S.3.3 in the electronic supplementary information. The provided images depict the original structure of the analyzed WO_3 sample as well as the structure of metallic tungsten powder after being heated up to 2400 °C. Further SEM images illustrating the initial structure of powders of APT[47], W[48] and WC[49] can be found in the literature.

View Article Online
DOI: 10.1039/D6JA00173D

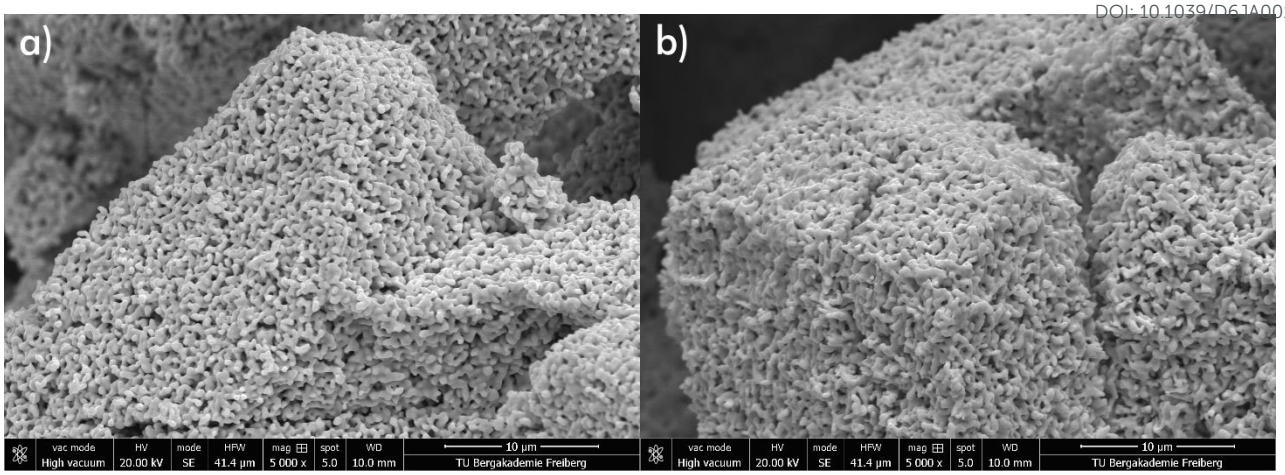

Figure 5: SEM images of APT (a) and WO_3 (b) after being heated to 2400 °C using H_2 as a modifier gas (SE mode, magnitude 5000x)

Calibration

Since the matrix is not evaporated, the calibration does not necessarily need matrix-analogous standards and this can also be done by graphite standards or dried aqueous standards solutions.[42] However, it was observed that the coefficient of determination was significantly low ($R^2 < 0.980$) when graphite standards were used since the evaporation of the analytes is incomplete without using a halogenated modifier. Therefore, the applicability of dries aqueous standard solutions was tested. In case of phosphorous and sulfur, coefficients of determination above 0.997 were achieved as it is shown in figure 6. For arsenic and manganese, coefficients above 0.990 were obtained. A little more problematic were aluminium, boron and silicon since they have a higher tendency to accumulate inside the graphite furnace under reducing conditions with hydrogen as the reaction gas. For these elements, coefficients of determination above 0.980 were observed. The correction model using the emission line of argon, introduced by Vogt *et al.*[45] for the correction of oxygen signals in coal samples can be applied here as well, but does not lead to a significant increase of the coefficients of determination.

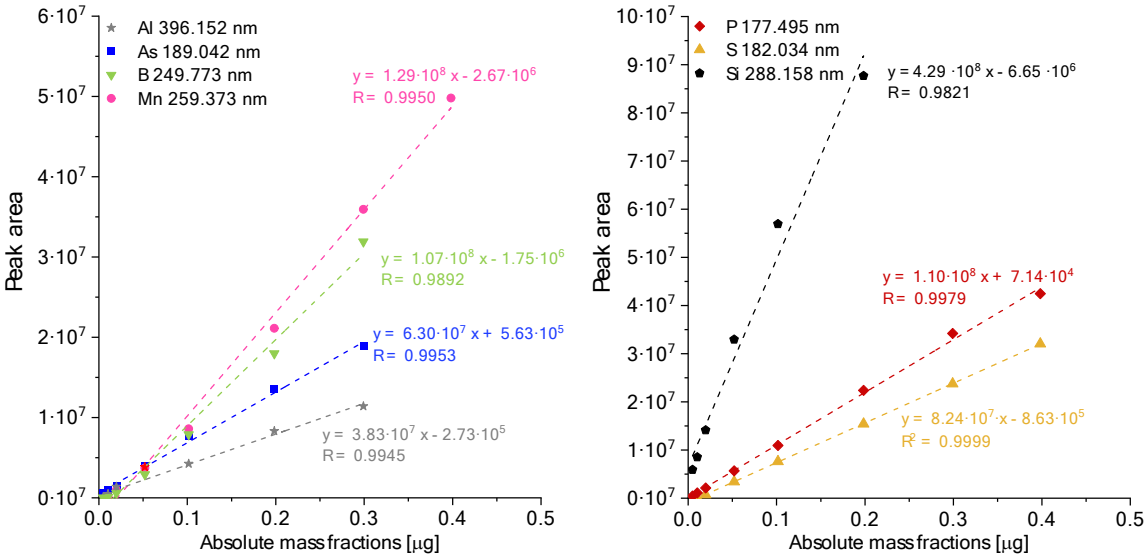

Figure 6: ETV-ICP-OES calibration of the selected elements based on dried aqueous standard solutions (corresponding elements and wavelengths in the left upper corner)

View Article Online
DOI: 10.1039/D6JA00173D

The only element, which could not be calibrated using dried aqueous standard solutions, was oxygen in tungsten and tungsten carbide. A suitable reference material is calcium oxalate monohydrate, which is already widely used for calibration in thermogravimetry.[43] With an inert atmosphere, usually provided by nitrogen, the compound is heated up to 900°C, where it decomposes in several individual steps depending on the temperature (see reaction scheme 1 and fig. 7).

$$CaC_2O_4 \cdot H_2O \xrightarrow{180\ °C} CaC_2O_4 \xrightarrow{490\ °C} CaCO_3 \xrightarrow{750\ °C} CaO \quad (1)$$

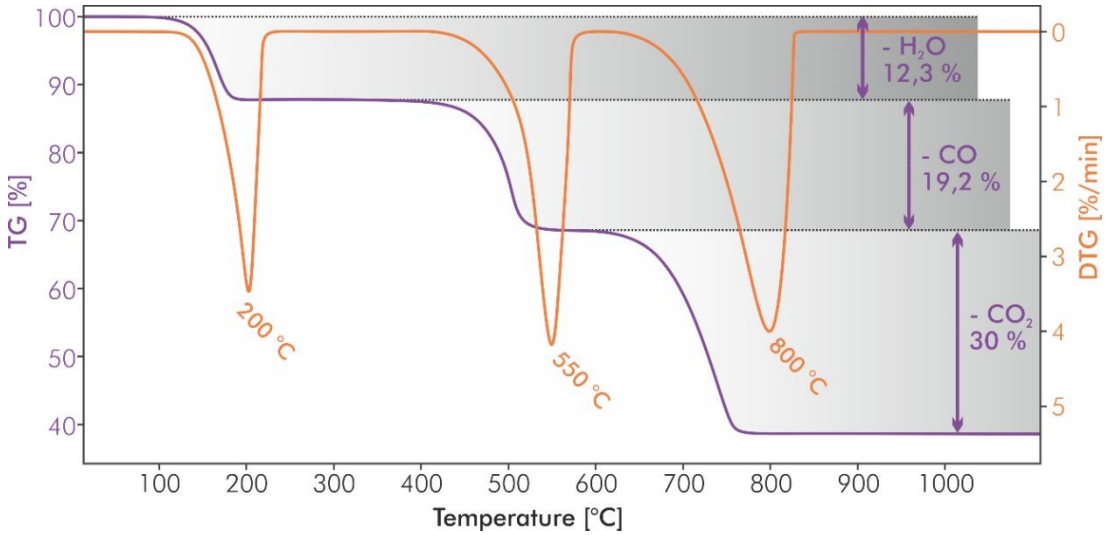

Figure 7: Evaporation of pure $CaC_2O_4 \cdot H_2O$ in TG/DTG in an inert atmosphere (nitrogen, 100 mL·min^{-1})

This calibration method was be extended to ETV-ICP-OES by Vogt *et al.*[42] to analyze the oxygen content in coal samples with CCl_2F_2 as a modifier gas. By evaporating high-purity calcium oxalate monohydrate in the graphite furnace, the same three peaks as on TGA can be observed in ETV-ICP-OES (see fig. 8). The additional fourth peak represents the vaporization of the calcium oxide, which is not seen in TGA. This example also shows that the ETV is capable of decomposition and species analysis using suitable conditions as demonstrated by Vogt *et al.*[44,46] for the speciation of oxygen in coal samples. Using H_2 as a modifier, the same peaks can be observed at slightly elevated temperatures due to the absence of reaction partners to form highly volatile halides (see fig. 8).

View Article Online
DOI: 10.1039/D6JA00173D

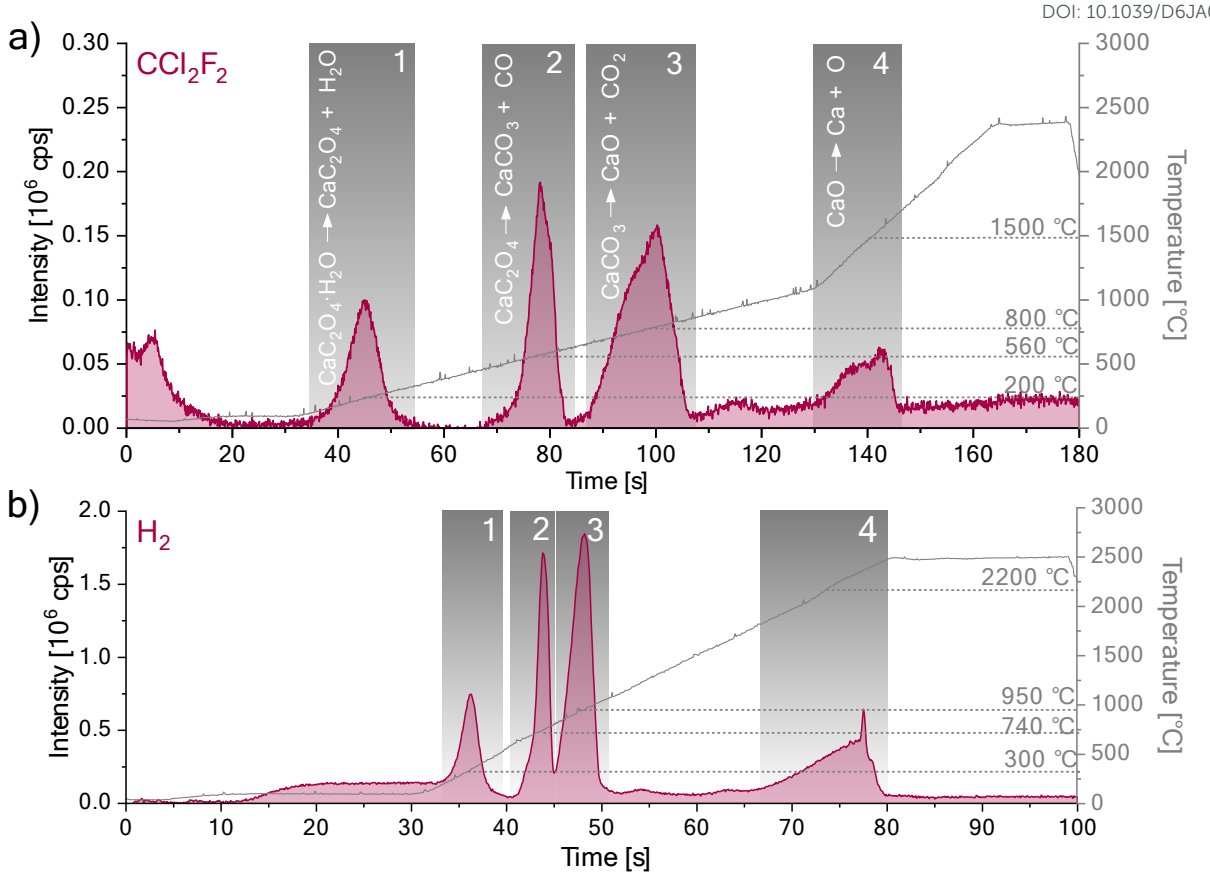

Figure 8: Evaporation of pure $CaC_2O_4 \cdot H_2O$ in ETV-ICP-OES with a) CCl_2F_2 as a modifier gas (adapted from [46]) and b) H_2 as modifier gas in ETV-ICP-OES (Peak 1: Release of crystal water, Peak 2: Decomposition of oxalate into carbonate and CO, Peak 3 – Decomposition of carbonate into oxide and CO_2, Peak 4- vaporization of oxide)

To obtain a calibration curve, six graphite boats were loaded with 0.1 to 1 mg Calcium oxalate monohydrate ($CaC_2O_4 \cdot H_2O$). It should be noted that within the chosen integration range, only four of the five oxygen atoms are released. This results in an oxygen content of 43.80 % in the standard. Due to the low initial mass and the statistical error of the scales the coefficient of determination of the calibration is comparatively low (see fig. 9).

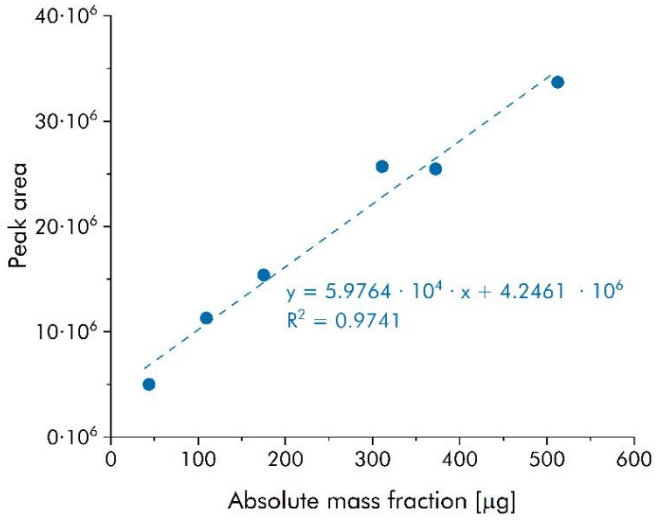

Figure 9: ETV-ICP-OES calibration of oxygen (130.603 nm) based on $CaC_2O_4 \cdot H_2O$

View Article Online
DOI: 10.1039/D6JA00173D

Rather than using an external calibration curve based on liquid standards, the standard addition method can be applied. This procedure was carried out exemplary for APT, WO_3 and W. Known amounts of the analyte are added directly to the sample within the graphite boat, after which the change in the measurement signal is observed. The resulting calibration curves, as shown in figure 10 for P and S (see fig. S.4 in the electronic supplementary information for Al, As, B, Mn, O, and Si), can then be used to determine the amount of analyte in a sample. However, this procedure is much more elaborate than external calibration, since each sample needs to be analyzed both alone and with several added amounts of standard solutions. Furthermore, several values in the range of 0.980 to 0.990 can be observed, which is comparatively low. This is caused by homogeneity issues within the samples. Only 10 mg of APT, WO_3 and W could be added to ensure the amount of analytes remained within the detector range after performing the standard addition procedure. In order to analyze higher sample quantities and compensate for homogeneity issues, it is recommended that the external calibration procedure be employed.

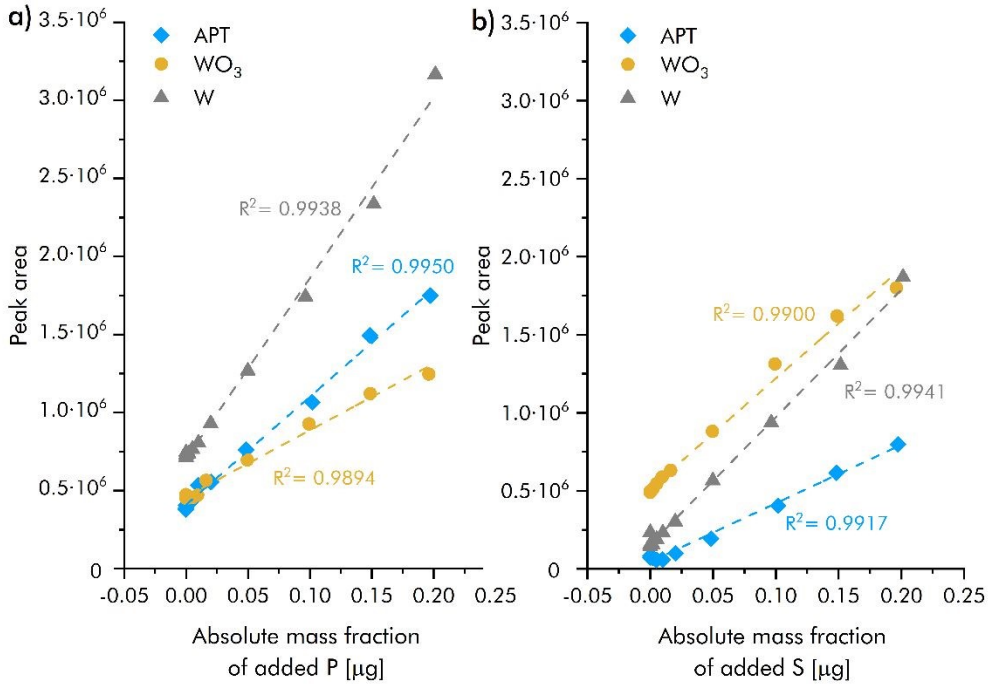

Figure 10: Calibration curves for the emission lines of phosphor at 177.495 nm (a) and sulfur at 182.034 nm (b) obtained after the addition of liquid standards to selected samples of APT

Statistical Analysis

The limits of detection were calculated according to DIN 32645[50], as outlined in previous studies.[51] They are located between 5 and 100 ppb, depending on the element, (see tab. 3) for those being calibrated with ICP-standard solutions. Calcium oxalate monohydrate contains 54.7 % oxygen, whereby only 43.8 % are released within the integration interval. This results in limits of detection of about 220 ppm for the emission line at 130.603 nm and about 380 ppm for the emission line at 130.485 nm, which is comparatively high for the method.

View Article Online
DOI: 10.1039/D6JA00173D

Table 3: Limits of detection (LOD) and quantification (LOQ) of all selected elements, calculated for a sample weight of 25 mg

Element	Wavelength [nm]	LOD [ppb]	LOQ [ppb]	Alternative wavelength [nm]	LOD [ppb]	LOQ [ppb]
Al	396.152	56.0	215.1	167.078	42.1	161.8
As	189.042	67.1	254.3	228.812	58.3	221.0
B	249.773	18.7	71.9	249.677	26.9	103.3
Mn	259.373	9.9	38.1	260.569	11.2	43.2
P	177.495	26.7	98.8	213.618	28.9	107.7
S	182.034	85.0	324.4	180.731	95.5	364.8
Si	288.158	65.1	220.1	251.612	55.5	187.4
O	130.603	219.9 ppm	720.3	130.485	377.8 ppm	1238.0

Since no certified reference materials were available in powder form at the time the study was conducted, an in-house standard with a given S-content was used instead to evaluate precision and trueness. According to the manufacturer, the sulfur content of two of the WO_3-samples was determined at 150 ppb and 7 ppm via glow discharge mass spectrometry (GD-MS). Further elemental contents were not given. Since the content at 150 ppb was below the calculated limit of quantification (see tab. 3), a statistical analysis was only possible for the sample with 7 ppm of sulfur. Due to severe interference caused by tungsten emission lines, digesting the samples and analyzing the resulting liquid after filtration of the remaining tungsten phases yielded no useful element content.

The results are shown in table 4 and figure 11. Trueness is roughly evaluated based on the recovery rates and the precision is given as the standard deviation (s) and the relative standard deviation (RSD) for each day, respectively. The Box-and-Whisker-Plot (see. fig. 11) shows outliers that were removed to calculate the mass fractions, standard deviations and recovery rates. Additionally, the stability of the measurements taken on different days is presented with n as the number of replicate measurements. It should be noted that day 1 to 4 all fell within a one-month period, with day 5 occurring more than a year later.

Table 4: Comparison of sulfur concentrations determined in this study with an in-house WO_3 reference material with a sulfur content of 7 ppm (25 mg sample weight)

Day	Mass fraction [mg·kg^{-1}]	s [mg·kg^{-1}]	RSD [%]	n	Recovery Rate [%]	s [%]
1	7.05	0.75	10.68	20	100.78	10.76
2	7.15	0.81	11.37	10	102.14	11.61
3	7.05	0.02	0.34	2	100.67	0.34
4	7.46	0.54	7.17	5	106.62	7.65
5	7.06	0.90	12.68	5	100.86	12.79

View Article Online
DOI: 10.1039/D6JA00173D

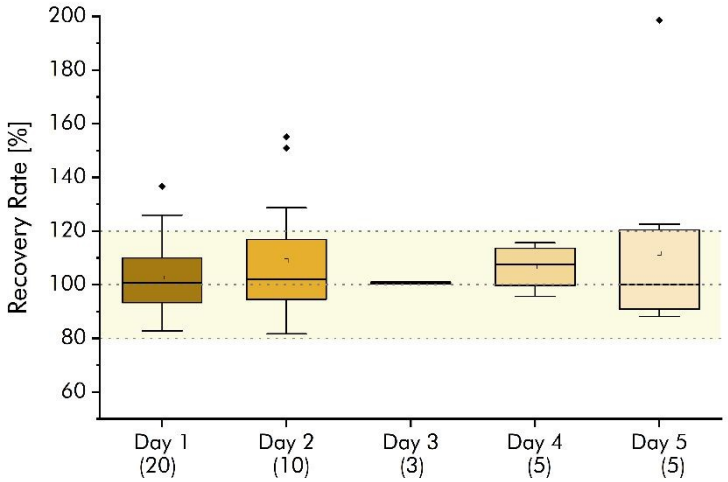

Figure 11: Box-and-Whisker-Plots of the recovery rates of sulfur (determined with the emission line at 182.034 nm) with an in-house WO_3 reference material with a sulfur content of 7 ppm at different days of analysis (25 mg sample weight, number of measurements given in brackets below on the x-axis)

Recoveries were predominantly obtained in the range of 80–120 % (see. fig. 11) and precision was lower than 15 % relative standard deviation (RSD, see tab. 4). Values above or below this range, especially outliers, are caused by inhomogeneities within the in-house reference material. The precision is comparable to that of other ETV-ICP-OES studies.[28,30,45,46,52] Furthermore, no significant differences between measurements taken on different days could be observed. In summary, this direct sampling method achieves adequate accuracy and fulfills the expectations of an analytical methods for process-accompanying characterization since information can be obtained with a measurement time of two minutes per sample.

Several samples of ammonium paratungstate ($(NH_4)_{10}(H_2W_{12}O_{42}) \cdot 4\ H_2O$; APT), blue tungsten oxide (WO_{3-x}), yellow tungsten oxide (WO_3), metallic tungsten (W) and tungsten carbide (WC) were analyzed using the developed method.

It was observed that the mass fractions of samples of two different manufacturers, that will be called A and B hereinafter, were showing significant differences concerning the contaminants. These are presumably based on different ore mining areas and manufacturing processes. This was chemometrically determined using a Student's t-test, where mean values of two samples are checked for significant differences.[53] The necessary values are calculated according to eq. 1. Here, x_A and x_B represent the mean values of the specific element contents in the samples from manufacturer A and manufacturer B, respectively. The values n_A and n_B describe the number of respective samples, and s_d describes the weighted average standard deviation. The latter can be calculated using eq. 2. The parameters are presented in table 5.

$$t = \frac{|\overline{x_A} - \overline{x_B}|}{s_d} \sqrt{\frac{n_A \cdot n_B}{n_A + n_B}} \quad (1)$$

$$s_d = \sqrt{\frac{(n_A - 1) \cdot s_A^2 + (n_B - 1) \cdot s_B^2}{n_A + n_B - 2}} \quad (2)$$

View Article Online
DOI: 10.1039/D6JA00173D

$$f = n_A + n_B - 2 \quad (3)$$

The null hypothesis ($\overline{x_A} - \overline{x_B} = 0$) was considered to be fulfilled if the mean values do not differ significantly, i.e., if the calculated t-value was smaller than the critical t-value $t_{(f;\,1-\frac{\alpha}{2})}$. If this was not the case, the alternative hypothesis ($\overline{x_A} - \overline{x_B} \neq 0$) was considered to be fulfilled. The significance level *α* was set at 0.05 here, and the number of degrees of freedom f was calculated using eq. 3. The critical t-values are tabulated in the literature.[53] Element contents below the detection limit were included in the calculation as 0 ppm.

Table 5: Values and intermediate results required to calculate the t-values for each element in the different samples depending on the manufacturer (t-values indicating significant differences are bolded)

Sample	APT	WO_{3-x} + WO_3	WO_3	W	WC
n_A	6	7	6	4	0
n_B	4	7	5	2	2
f	8	12	9	4	-
$t_{(f;\,1-\frac{0,05}{2})}$	1.860	1.782	1.833	2.132	-
t-values					-
Al	1.058	1.519	**1.898**	1.895	-
As	**7.683**	**2.395**	**4.600**	**2.895**	-
B	-*	**3.068**	**7.424**	-*	-
Mn	-*	1.419	**1.981**	0.115	-
P	**3.778**	0.964	1.051	**2.529**	-
S	**3.744**	0.334	0.445	0.355	-
Si	**3.790**	0.641	0.304	1.797	-

* determined mass fractions of all samples < LOQ

In ammonium paratungstate samples, the elements As, P, S and Si are to be regarded as significantly different. In tungsten oxides this concerns the elements As and B. If only the yellow tungsten oxides are taken into account, the differences extend to Al and Mn. In metallic tungsten samples the elements As and P are to be regarded as significantly different. A t-test for WC could not be carried out since only samples of one manufacturer were available.

Conclusions

With the help of H_2 as a suitable modifier gas, optimized plasma parameters and a temperature program up to 2450 °C, intermediate and end products along the production process of tungsten can be analyzed by ETV-ICP-OES. If only the intermediates ammonium paratungstate and the tungsten oxides are used as samples, a maximum temperature of 2000 °C is sufficient to evaporate the analytes. Elements of interest are Al, As, B, Mn, O, P, S and Si, although the method can be extended to all practically relevant elements.

When using hydrogen as a modifier gas, only the analytes are evaporated, while the tungsten matrix remains in the graphite boats of the ETV. Therefore, the lack of matrix-analogues reference materials can be compensated by calibrating outside the matrix. For the majority of the chosen elements, the calibration can be

View Article Online
DOI: 10.1039/D6JA00173D

performed by using dried aqueous standard solutions, which significantly improves the versatility of the ETV-ICP-OES. Oxygen can be calibrated with calcium-oxalate monohydrate.

For the analysis, a sample mass of approximately 25 mg was found to be useful. In case of high element concentrations, the initial weight can be lowered to 5 mg. Since the analysis takes about 2 minutes per sample and next to no sample preparation is necessary, a high repetition rate is possible without much effort. To compensate homogeneity issues or to generate lower limits of detection, the sample mass can also be increased up to 40 mg. The limits of detection amongst the elements, which were calibrated by using dried aqueous standard solutions, were determined between 10 and 100 ppb when 25 mg of tungsten samples were analyzed. In case of oxygen, the LOD was to be found between 200 and 400 ppm. The limits of detection can be further decreased by operating the system inside a clean room or a laminar flow box.

View Article Online
DOI: 10.1039/D6JA00173D

Author contributions according to CRediT

D. Friebel: conceptualization, investigation, methodology, formal analysis, visualization, writing – original draft, review & editing

T. Vogt: project administration, investigation, methodology, conceptualization, writing – review & editing

C. Vogt: project administration, supervision, writing – review & editing

Conflicts of interest

The authors declare no conflict of interest.

Data availability

Data for this article, including the ETV-ICP-OES spectra are available at Zenodo at https://doi.org/10.5281/zenodo.20121163.

Acknowledgements

The authors would like to thank the Institute of Energy Process Engineering and Chemical Engineering (IEC) of TU Bergakademie Freiberg for the cooperation in carrying out the SEM measurements. There was no AI tool involved in creating this research paper.

References

1 K. Cammann, Instrumentelle analytische Chemie. Verfahren, Anwendungen und Qualitätssicherung, Spektrum Akademischer Verlag, Heidelberg, 2001, DOI 10.1007/978-3-8274-2740-3.
2 M. Balcerzak, Sample digestion methods for the determination of traces of precious metals by spectrometric techniques, *Anal. Sci.*, 2002, **18**, 737–750. DOI: 10.2116/analsci.18.737.
3 J. Sneddon, C. Hardaway, K. K. Bobbadi and A. K. Reddy, Sample Preparation of Solid Samples for Metal Determination by Atomic Spectroscopy—An Overview and Selected Recent Applications, *Applied Spectroscopy Reviews*, 2006, **41**, 1–14, DOI: 10.1080/05704920500385445.
4 A. F. Holleman, E. Wiberg and N. Wiberg, Anorganische Chemie, de Gruyter, Berlin, 103rd edn., 2017, DOI: 10.1515/9783110206845.
5 H. Danninger, A. Atari, B. Lux, E. Kny and A. Tschulik, Embrittlement of tungsten heavy alloys by trace impurities and their analytical characterization, *Z. Anal. Chem.*, 1989, **333**, 417–421, DOI: 10.1007/BF00572341.
6 M. Archer, R. I. McCrindle and E. R. Rohwer, Analysis of cobalt, tantalum, titanium, vanadium and chromium in tungsten carbide by inductively coupled plasma-optical emission spectrometry, *J. Anal. At. Spectrom.*, 2003, **18**, 1493–1496, DOI: 10.1039/b310482f.
7 T. W. Penrice, in *Kirk-Othmer Encyclopedia of Chemical Technology*, ed. R. E. Kirk and D. F. Othmer, Wiley, New York, 2013, DOI 10.1002/0471238961.2021140716051418.a02.pub3.
8 L. B. Ekbom, The distribution and influence of impurities in tungsten heavy metals, *Int. J. Refract. Met. Hard Mater.*, 1991, **10**, 155–159, DOI: 10.1016/0263-4368(91)90020-O.
9 G. L. Krasko, Effect of impurities on the electronic structure of grain boundaries and intergranular cohesion in iron and tungsten, *Mater. Sci. Eng.*, 1997, **234-236**, 1071–1074, DOI: 10.1016/S0921-5093(97)00417-6.
10 Z. Pan, L. J. Kecskes and Q. Wei, The nature behind the preferentially embrittling effect of impurities on the ductility of tungsten, *Comput. Mater. Sci.*, 2014, **93**, 104–111, DOI:

View Article Online
DOI: 10.1039/D6JA00173D

10.1016/j.commatsci.2014.06.036.
11 E. Lassner and W.-D. Schubert, Tungsten. Properties, chemistry, technology of the elements, alloys and chemical compounds, Kluwer Academic, New York, London, 1999, DOI: 10.1007/978-1-4615-4907-9.
12 M. Bertau, A. Müller, P. Fröhlich and M. Katzberg, Industrielle anorganische Chemie, Wiley-VCH, Weinheim, 4th edn., 2013, DOI: 10.1002/9783527649563.
13 Y. Cheng, Determination of alloy and impurity elements in the WC-Co based cemented carbide by microwave digestion - inductively coupled plasma atomic emission spectrometry, *Appl. Mech. Mater.*, 2013, **271-272**, 222–226, DOI: 10.4028/www.scientific.net/AMM.271-272.222.
14 P. C. Mürau, Dissolution of Tungsten by Hydrogen Peroxide, *Anal. Chem.*, 1961, **33**, 1125–1126, DOI: 10.1021/ac60176a021.
15 P. C. Mürau, Resolution of tungsten with hydrogen peroxide, *Chem. Zentralbl.*, 1961, **132**, 17136.
16 V. Krivan and K.-H. Theimer, Trace characterization of high-purity molybdenum and tungsten by electrothermal atomic absorption spectrometry, inductively coupled plasma atomic emission spectrometry, inductively coupled plasma mass spectrometry and total reflection X-ray fluorescence spectrometry involving analyte—matrix separation, *Spectrochim. Acta, Part B*, 1997, **52**, 2061–2076, DOI: 10.1016/S0584-8547(97)00105-5.
17 A. Leclercq, A. Nonell, J. L. Todolí Torró, C. Bresson, L. Vio, T. Vercouter and F. Chartier, Introduction of organic/hydro-organic matrices in inductively coupled plasma optical emission spectrometry and mass spectrometry: a tutorial review. Part II. Practical considerations, *Anal. Chim. Acta*, 2015, **885**, 57–91.
18 S. Liu, Z. Han, X. Kong, J. Zhang, Z. Lv and G. Yuan, Organic matrix effects in inductively coupled plasma mass spectrometry: a tutorial review, *Appl. Spectrosc. Rev.*, 2022, **57**, 461–489.
19 S. Natansohn and G. Czupryna, Determination of impurities in industrial products by d.c. plasma emission spectrometry, *Spectrochim. Acta, Part B*, 1983, **38**, 317–322, DOI: 10.1016/0584-8547(83)80130-X.
20 J. F. Cosgrove and G. H. Morrison, Activation analysis of trace impurities in tungsten by using scintillation spectrometry, *Anal. Chem.*, 1957, **29**, 1017–1019, DOI: 10.1021/ac60127a006.
21 S. Hasegawa, Determination of Trace Elements in High Purity Tungsten by Solid-Phase Extraction/ICP-MS, *Mater. Trans.*, 2008, **49**, 2054–2057, DOI: 10.2320/matertrans.MRA2008135.
22 M. Otto, Analytische Chemie, Wiley-VCH, Weinheim, 4th edn., 2011, DOI: 10.1002/9783527344659.
23 D. Vogt, T. Vogt and M. Otto, in *Stoffliche Nutzung von Braunkohle*, ed. S. Krzack, H. Gutte and B. Meyer, Springer Vieweg, Berlin, Heidelberg, 2018, pp. 86–100, DOI: 10.1007/978-3-662-46251-5.
24 S. Recknagel, S. Richter, F. Reinholdsson, J. Pettersson and I. Gustavsson, An Intercomparison Study of Analytical Methods for the Determination of Magnesium in Low Alloy Steel, *Steel Res. Int.*, 2012, **83**, 146–149, DOI: 10.1002/srin.201100187.
25 M. Resano, E. García-Ruiz, K. S. McIntosh, J. Hinrichs, I. Deconinck and F. Vanhaecke, Comparison of the solid sampling techniques laser ablation-ICP-MS, glow discharge-MS and spark-OES for the determination of platinum group metals in Pb buttons obtained by fire assay of platiniferous ores, *J. Anal. At. Spectrom.*, 2006, **21**, 899–909, DOI: 10.1039/B603270B.
26 A. A. Ganeev, A. R. Gubal, K. N. Uskov and S. V. Potapov, Analytical glow discharge mass spectrometry, *Russ. Chem. Bull.*, 2012, **61**, 752–767, DOI: 10.1007/s11172-012-0107-5.
27 J. Becker and H.-J. Dietze, State-of-the-art in inorganic mass spectrometry for analysis of high-purity materials, *Int. J. Mass Spectrom.*, 2003, **228**, 127–150, DOI: 10.1016/S1387-3806(03)00270-7.
28 J. Hassler, R. Matschat, S. Richter, P. Barth, A. K. Detcheva and H.-J. Waarlo, Determination of 22 trace elements in high-purity copper including Se and Te by ETV-ICP OES using SF_6, NF_3, CF_4 and H_2 as chemical modifiers, *J. Anal. At. Spectrom.*, 2016, **31**, 642–657, DOI 10.1039/C5JA00240K.
29 J. Hassler, P. Barth, S. Richter and R. Matschat, Determination of trace elements in high-purity copper by ETV-ICP OES using halocarbons as chemical modifiers, *J. Anal. At. Spectrom.*, 2011, **26**, 2404–2418, DOI: 10.1039/c1ja10149h.
30 C. Hommel, J. Hassler, R. Matschat, T. Vogt, A. K. Detcheva and S. Recknagel, A fast and robust direct solid sampling method for the determination of 27 trace, main and minor elements in soda-lime glass based on ETV-ICP OES and using a gaseous halogenating modifier, *J. Anal. At. Spectrom.*, 2021, **36**, 1683-1693, DOI: 10.1039/d1ja00081k.
31 K. C. Friese, U. Wätjen and K. H. Grobecker, Analyte transport efficiencies in electrothermal

View Article Online
DOI: 10.1039/D6JA00173D

vaporization for inductively coupled plasma mass spectrometry, *Fresenius' J. Anal. Chem.*, 2001, **370**, 843–849, DOI: 10.1007/s002160100865.

32 J. Mierzwa and M. Yang, Electrothermal vaporization–inductively coupled plasma mass spectrometry for determination of metal impurities in slurries of aluminium oxide, *J. Anal. At. Spectrom.*, 1998, **13**, 667–671, DOI: 10.1039/A801207E.

33 B. U. Peschel, F. Andrade, W. C. Wetzel, G. D. Schilling, G. M. Hieftje, J. A. Broekaert, R. Sperline, M. B. Denton, C. J. Barinaga and D. W. Koppenaal, Electrothermal vaporization coupled with inductively coupled plasma array–detector mass spectrometry for the multielement analysis of Al_2O_3 ceramic powders, *Spectrochim. Acta, Part B*, 2006, **61**, 42–49, DOI: 10.1016/j.sab.2005.11.007.

34 M. C. Wende and J. Broekaert, Direct solid sampling electrothermal vaporization of alumina for analysis by inductively coupled plasma optical emission spectrometry, *Spectrochim. Acta, Part B*, 2002, **57**, 1897–1904, DOI: 10.1016/S0584-8547(02)00212-4.

35 S. Zhou, L. Fu and B. Liang, Clustering analysis of ancient celadon based on SOM neural network, *Sci. China Ser. E-Technol. Sci.*, 2008, **51**, 999–1007, DOI: 10.1007/s11431-008-0086-9.

36 P. Barth, J. Hassler, I. Kudrik and V. Krivan, Determination of trace impurities in boron nitride by graphite furnace atomic absorption spectrometry and electrothermal vaporization inductively coupled plasma optical emission spectrometry using solid sampling, *Spectrochim. Acta, Part B*, 2007, **62**, 924–932, DOI: 10.1016/j.sab.2007.03.012.

37 Y. Okamoto, H. Kataoka, S. Tsukahara and T. Fujiwara, Sequential determination of boric acid and boron nitride by electrothermal vaporisation inductively coupled plasma atomic spectrometry, *J. Anal. At. Spectrom.*, 2005, **20**, 383, DOI: 10.1039/b501116g.

38 G. Záray, F. Leis, T. Kántor, J. Hassler and G. Tölg, Analysis of silicon carbide powder by ETV-ICP-AES, *Fresenius' J. Anal. Chem.*, 1993, **346**, 1042–1046, DOI: 10.1007/BF00323713.

39 J. Hassler, G. Záray, K. Schwetz and K. Flórián, Speciation of aluminium in silicon carbide by electrothermal vaporization-inductively coupled plasma atomic emission spectrometry, *J. Anal. At. Spectrom.*, 2005, **20**, 954–956, DOI: 10.1039/b504613k.

40 R. Matschat, J. Haßler, H. Traub and A. Dette, Multielement trace determination in SiC powders, *Anal. Bioanal. Chem.*, 2005, **383**, 1060–1074, DOI: 10.1007/s00216-005-3415-x.

41 T. Bacquart, J. Hassler, T. Vogt, P. Perzl, S. Steigerwald, W. Schmidt, M. Sterckx and T. P. J. Linsinger, ETV-ICP-OES, *Accredit. Qual. Assur.*, 2017, **22**, 125–139, DOI: 10.1007/s00769-017-1254-z.

42 A. Detcheva, P. Barth and J. Hassler, Calibration possibilities and modifier use in ETV ICP OES determination of trace and minor elements in plant materials, *Anal. Bioanal. Chem.*, 2009, **394**, 1485–1495, DOI: 10.1007/s00216-009-2835-4.

43 N. Kutaish, P. Aggarwal and D. Dollimore, Thermal analysis of calcium oxalate samples obtained by various preparative routes, *Thermochim. Acta*, 1997, **297**, 131–137, DOI: 10.1016/S0040-6031(97)00002-6.

44 D. Vogt, T. Vogt, B. Wolf, M. Neuroth and M. Otto, Direct determination of organic and inorganic oxygen in coals from the Argonne Premium sample program by solid sampling electrothermal vaporization inductively coupled plasma optical emission spectrometry, *Fuel*, 2017, **196**, 185–194.

45 T. Vogt, D. Bauer, M. Neuroth and M. Otto, Quantitative multi-element analysis of Argonne Premium Coal samples by ETV-ICP OES – A highly efficient direct analytical technique for inorganics in coal, *Fuel*, 2015, **152**, 96–102, DOI: 10.1016/j.fuel.2014.12.057.

46 T. Vogt, D. Bauer, D. Nennstiel and M. Otto, Solid-Sampling Electrothermal Vaporization Inductively Coupled Plasma Optical Emission Spectrometry for Direct Determination of Total Oxygen in Coal, *Anal. Chem.*, 2015, **87**, 10414–10420, DOI: 10.1021/acs.analchem.5b02530.

47 M. Sadeghi, S. Rezaee, A. Arman, Ş. Ţălu, C. Luna and R. Shakoury, Study of the formation of tungsten powder by hydrogen reduction of ammonium paratungstate and stereometric analyses of the powder texture, *Mater. Res. Express*, 2019, **6**, 1265f7, DOI: 10.1088/2053-1591/ab6763.

48 K. Raj, Effect of WO_3 powder particle shape, size and bulk density, on the grain size and grain size distribution of tungsten metal powder, *Metal Powder Report*, 2016, **71**, 285–287, DOI: 10.1016/j.mprp.2016.05.007.

49 G. Mühlbauer, G. Kremser, A. Bock, J. Weidow and W.-D. Schubert, Transition of W 2 C to WC during carburization of tungsten metal powder, *Int. J. Refract. Hard Met.*, 2018, **72**, 141–148, DOI:

View Article Online
DOI: 10.1039/D6JA00173D

10.1016/j.ijrmhm.2017.12.018.

50 Deutsches Institut für Normung e. V., *DIN 32645:2008-05: Chemical analysis- Decision limit, detection limit and determination limit under repeatability conditions - Terms, methods, evaluation*, Beuth Verlag GmbH, Berlin, 32645th edn., 2008, **ICS 71.040.01.**

51 D. Friebel, T. Pietschner, T. Vogt and C. Vogt, Direct process accompanying analysis of plant-based biomass samples for critical elements in combusting processes with ETV-ICP-OES, *Biomass Futures*, 2026, **1**, 100027, DOI: 10.1016/j.bmf.2026.100027.

52 A. Limbeck, M. Bonta and W. Nischkauer, Improvements in the direct analysis of advanced materials using ICP-based measurement techniques, *J. Anal. At. Spectrom.*, 2017, **32**, 212–232, DOI: 10.1039/C6JA00335D.

53 M. Otto, Chemometrics: statistics and computer application in analytical chemistry, Wiley, Weinheim, New York, 3rd edn., 2016, DOI: 10.1002/9783527699377.

Data Availability according to the manuscript – “Process-accompanying analysis of solid intermediate and end products in the manufacturing process of high-purity tungsten by ETV-ICP-OES”

Data for this article, including the ETV-ICP-OES spectra are available at Zenodo at https://doi.org/10.5281/zenodo.20121163.